RSC Advances

PAPER

View Article Online
View Journal | View Issue

Cite this: *RSC Adv.*, 2015, **5**, 22703

Enantioselective bioreductive preparation of chiral halohydrins employing two newly identified stereocomplementary reductases†

Guo-Chao Xu,[ab] Hui-Lei Yu,*[a] Yue-Peng Shang[a] and Jian-He Xu*[a]

Received 21st December 2014
Accepted 9th February 2015

DOI: 10.1039/c4ra16779a

www.rsc.org/advances

Two robust stereocomplementary carbonyl reductases (*Dh*CR and *Cg*CR) were identified through rescreening the carbonyl reductase toolbox. Five reductases were returned through the activity and enantioselectivity assay for α-chloro-1-acetophenone and ethyl 4-chloro-3-oxo-butanate (COBE). Three reductases were stable at elevated substrate loading. Enzymatic characterization revealed that *Dh*CR and *Cg*CR were more thermostable. As much as 330 g COBE in 1 L biphasic reaction mixture was reduced to (*S*)- and (*R*)-3-hydroxy-4-chlorobutyrate by *Dh*CR and *Cg*CR (coexpressed with glucose dehydrogenase), with 92.5% and 93.0% yields, >99% ee, and total turnover numbers of 53 800 and 108 000, respectively. Six other α-halohydrins were asymmetrically reduced to optically pure forms at a substrate loading of 100 g L^{-1}. Our results indicate the potential of these two stereocomplementary reductases in the synthesis of valuable α-halohydrins for pharmaceuticals.

Introduction

Asymmetric reduction of prochiral ketones is one of the most important fundamental and practical reactions for production of chiral secondary alcohols, which can be transformed into various functionalities of industrial relevance for pharmaceuticals, agrochemicals and natural products.[1] Optically active α-halogenated alcohols constitute important building blocks in the synthesis of pharmaceutical and liquid crystal products.[2] Most importantly, the two opposite enantiomers may have similar, different or even opposite effects. For example, ethyl (*S*)-3-hydroxy-4-chlorobutyrate ((*S*)-CHBE) is a key chiral precursor for HMG-CoA reductase inhibitors to lower cholesterol, whereas (*R*)-CHBE is an important intermediate for L-carnitine, which acts as an antioxidant.[3,4] Both enantiomers of 2-chloro-1-(2′,4′-dichlorophenyl)ethanol could be used in the synthesis of antifungal agents, such as miconazole, econazole, and sertaconazole, with different antifungal profiles and activities.[5] Hence, the enantioselective preparation of both α-halohydrins enantiomers is of equal importance.

The manufacturing industry is searching for efficient, green, energy-saving and environmentally benign procedures.[6] The discovery and application of biocatalysts for chemical synthesis, especially for value-added products, promise new synthetic methods due to their specialized and complicated spatial, electronic and polar structures.[7] The properties of enzymes mean that they are highly diverse and enantioselective, easy to use, environmentally benign and have a high atom economy.[8] Dramatic improvement has been achieved employing enzymes, accompanying the third wave of biocatalysis.[9]

Because of the demanding diversity in biomanufacturing, there is a constant need for new biocatalysts with altered performance, such as high catalytic efficiency, wide substrate scope, high regio- and enantioselectivity, thermo- and pH-stability and high tolerance to substrates, products, and organic solvents.[10] For specific reactions, classical enrichment cultivation is an effective strategy for identifying microorganisms harboring new active enzymes. Based on this, various new and efficient tools have been established to shorten the period for discovering enzymes with desired properties, including metagenomics, shotgun insertion, mutation, genome database mining, and isolation and purification approaches for the original microorganisms.[11] Recently, genome database mining, which allows the screening of enzymes with similar sequences through target-reaction-oriented screening and selection, has produced various breakthroughs. Recombinant DNA technology has enabled the rapid increase in accessible genome data (currently at a rate of about 200 genomes per month), providing more and more sequences with unknown functions and promoting the quick identification of naturally-evolved enzyme libraries by genome mining.[12] Various strategies have been published for the prediction and rational selection of

[a]*State Key Laboratory of Bioreactor Engineering, East China University of Science and Technology, and Shanghai Collaborative Innovation Center for Biomanufacturing Technology, Shanghai 200237, China. E-mail: huileiyu@ecust.edu.cn; jianhexu@ecust.edu.cn*

[b]*The Key Laboratory of Industrial Biotechnology, Ministry of Education, School of Biotechnology, Jiangnan University, Wuxi 214122, China*

† Electronic supplementary information (ESI) available. See DOI: 10.1039/c4ra16779a

genes from the genome database.[13] However, the focus has not been on strategies to identify robust enantioselective enzymes.

To work as an alternative to chemical synthesis on an industrial scale, one biocatalyst should possess certain properties, such as tolerance to a minimum of 100 g L^{-1} substrate, >99% enantioselectivity, high operational stability, no byproducts and cofactor addition of <0.1 g L^{-1}.[14] Our group has been involved in the discovery and engineering of robust enzymes with promising potential uses in organic synthesis of chiral building blocks with pharmaceutical relevance, as shown in Table 1. An NADH-dependent carbonyl reductase, *Sc*CR, has been identified from *Streptomyces coelicolor* with a substrate-coupled cofactor regeneration. Its specific production rate was 36.8 $g_{product}/g_{dry\text{-}cell\text{-}weight}$ in the asymmetric preparation of the key chiral precursor for atorvastatin (Lipitor).[15] For the synthesis of chiral *o*-chloromandelic acids, key building blocks for clopidogrel (Plavix), two biocatalysts, an NADPH-dependent ketoreductase, *Cg*KR1, and an novel nitrilase, *La*N, have been discovered in *Candida glabrata* and *Labrenzia aggregata*, respectively.[16,23] Their space-time yield reached >100 g L^{-1} day^{-1} for the asymmetric reduction of methyl *o*-chlorobenzoylformate (CBFM) and enantioselective resolution of *o*-chloromandelonitrile (CMN), respectively. However, based on our previous results in genome mining, as shown in Table 1, one biocatalyst with desired characteristics was obtained from 8–30 candidates (rejection rate of >87.5%). Nonetheless, most of the genes were not investigated and little is known about their properties because a single screen was run and the selection criteria were generally limited to activity and enantioselectivity towards the target substrate. In our previous work, only one substrate-tolerant carbonyl reductase *Kt*CR was screened out of 30 potential reductases for preparing chiral halohydrins from α-chloro-1-acetophenone (CAPE, **4**).[18] We expected that the other reductases might display similar or even higher catalytic performance. To rescreen this library for robust reductases, three further rounds of screening were proposed, covering activity and enantioselectivity for substrates with altered substituents as primary screening, operational stability against substrate/product and thermostability. The application potential in the enantioselective preparation of halohydrins was also investigated.

Results and discussion

Rescreening result with COBE substrate

A carbonyl reductase toolbox was developed for robust haloketone reductases. In our primary screening using **4** as the target substrate, only three carbonyl reductases (*Kt*CR, *Pg*CR and *Cl*CR) were returned with higher activity (>0.5 U mg^{-1}) and enantioselectivity (>99%).[18] Among them, the highest activity was determined with *Cl*CR (1.5 U mg^{-1}). Further comparison at increased substrate loading revealed the instability of *Pg*CR and *Cl*CR, and only *Kt*CR was selected (Table 2). Most of the candidates were eliminated due to their low activity. However, changing the screening substrate to ethyl 4-chloro-3-oxobutanate (COBE, **22**), an α-halogenated β-ketoester, resulted in a different profile (Fig. 1). Twelve reductases were identified with specific activity of more than 0.5 U mg^{-1}, which was higher than that with **4**. These exciting results encouraged us to analyze the enantioselectivity in the asymmetric reduction of **22** and **4**. *Dh*CR and *Cg*CR, from *Debaryomyces hansenii* (Uniprot accession no. Q6BQ25) and *Candida glabrata* (Q6FR42), respectively, displayed stable performance, even at 200 mM of **4** (Table 2). Particularly for *Dh*CR, the time and catalyst requirement was much less than for *Kt*CR, although the apparent specific activity of *Dh*CR was only 38% that of *Kt*CR, indicating that low apparent activity has little connection with the biotransformation efficiency. *Cg*CR was the only reductase with Prelog preference in the asymmetric reduction of prochiral ketones. Reductases with relatively higher activity were more liable to have unstable enantioselectivity. Harsh conditions, such as high reagent concentration (substrate or product) and high temperature, might affect the structural conformation of the enzyme and decrease their activity and enantioselectivity. Considering the activity and ee for two screening substrates, *Dh*CR and *Cg*CR were regarded as interesting reductases, in addition to *Kt*CR. Hence, for the primary screening for activity and operational stability in genome data mining, using at least

Table 1 Enzymes identified through genome data mining

	Enzyme	EC[a]	Candidate[b]	Characteristics: substrate, loading [g L^{-1}], ee [%], STY [g L^{-1} day^{-1}][c]	Ref.
1	*Sc*CR	1	10	COBE, 600, >99, 304	15
2	*Cg*KR1	1	8	CBFM, 300, >98.7, 261	16
3	*Cg*KR2	1	13	OPBE, 206, >99, 700	17
4	*Kt*CR	1	30	CAPE, 154, >99, 283	18
5	*Ar*QR	1	17	QNCO, 242, >99, 916	19
6	*Es*LeuDH	1	15	TMP, 78.1, >99, 275	20
7	*Ba*NTR1	1	24	CNB, 14.8, >99 sel., 291	21
8	rPPE01	3	17	APA, 64.8, 99, 97.2	22
9	*La*N	3	13	CMN, 50.2, 96.5, 143	23
10	*Ba*E	3	22	MDPEA, 40, 97, 38.6	24

[a] EC classification, 1 as oxidoreductase, 3 as hydrolase. [b] Numbers of candidates. [c] STY: space-time yield. Substrates: COBE (ethyl 4-chloro-3-oxobutanate), CBFM (methyl *o*-chlorobenzoylformate), OPBE (ethyl 3-oxo-phenylbutanate), CAPE (α-chloro-1-acetophenone) QNCO (3-quinuclidinone), CNB (4-cyanonitrobenzene), APA (α-acetoxyphenyl acetate), MDPEA (1-(3′,4′-methylenedioxyphenyl) ethyl ester), CMN (*o*-chloromandelonitrile).

Table 2 Asymmetric reduction of α-chloroacetophenone with the five best carbonyl reductases

Enzyme	Substrate [mM]	Catalyst [kU L^{-1}]	Time [h]	Conv. [%]	ee [%], *R*/*S*
*Cl*CR	10	1	12	>99	>99/*S*
	100	10	12	>99	95.6/*S*
	200	40	24	80.8	80.0/*S*
*Kt*CR	10	1	12	>99	>99/*S*
	100	10	12	>99	>99/*S*
	200	20	12	>99	>99/*S*
*Pg*CR	10	1	12	>99	>99/*S*
	100	10	12	>99	92.4/*S*
	200	40	24	76.6	60.5/*S*
*Dh*CR	10	1	6	>99	>99/*S*
	100	10	6	>99	>99/*S*
	200	10	6	>99	>99/*S*
*Cg*CR	10	1	12	>99	98.7/*R*
	100	10	12	>99	98.6/*R*
	200	20	8	>99	98.7/*R*

two substrates with similar structures was better for understanding the enzyme performance comprehensively. However, other characteristics, such as the substrate profiles toward different kinds of substrates and enzyme performance (thermostability), were also considered.

Enzymatic characteristics of three carbonyl reductases

Three recombinant reductases with an *N*-terminal His-tag were purified to electrophoretic homogeneity by nickel affinity chromatography. The specific activities toward **22** of purified *Dh*CR, *Kt*CR and *Cg*CR were 13, 11 and 8.0 U mg^{-1}, respectively. Protein separation of the purified enzyme by SDS-PAGE resulted in a single band for each enzyme, corresponding to a molecular weight of 34, 35 and 40 kDa, for *Dh*CR, *Kt*CR and *Cg*CR, respectively (Fig. S1†), in agreement with their theoretical values. Gel exclusion chromatography with a TSK G2000 SWx1 column showed a single peak for *Dh*CR, *Kt*CR and *Cg*CR with an elution volume corresponding to an apparent molecular mass of 67.2 69.6 and 39.8 kDa, respectively, which indicated that they were homodimeric and monomeric enzymes.

Table 3 Comparison of the enzymatic characteristics of *Kt*CR, *Dh*CR and *Cg*CR

Characteristic		*Kt*CR	*Dh*CR	*Cg*CR
Molecular weight [kDa]		69.8	67.2	39.8
Numbers of subunit		2	2	1
Optimal pH		6.5	6.5	6.5
Optimal temperature [°C]		45	55	60
Thermostability [h]	30 °C	18.0	462	169
	40 °C	11.8	111	80.6
	50 °C	0.163	2.09	1.26
Ea [kJ mol^{-1}]		190 ± 5	218 ± 6	198 ± 3
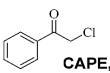 CAPE, 4	K_M [mM]	2.3 ± 0.2	2.1 ± 0.1	2.2 ± 0.1
	k_{cat} [s^{-1}]	7.3 ± 0.3	4.0 ± 0.2	1.6 ± 0.1
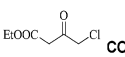 COBE, 22	K_M [mM]	3.2 ± 0.1	1.3 ± 0.1	3.7 ± 0.2
	k_{cat} [s^{-1}]	13.2 ± 0.2	16.6 ± 0.3	27.9 ± 0.4

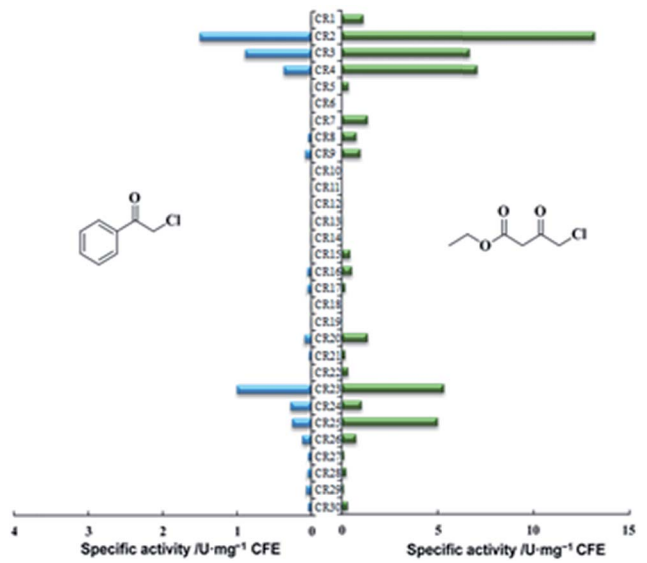

Fig. 1 Screening results for the 30 carbonyl reductases using two haloketones (**4** and **22**) with different substituents. Blue columns: activity towards CAPE, green columns: activity towards COBE.

The effect of pH and temperature on the activity of three carbonyl reductases was investigated (Fig. S2†). All displayed their highest activity at around pH 6.5. The optimum temperatures of *Dh*CR, *Cg*CR and *Kt*CR were 55, 60, and 45 °C, respectively, according to the temperature profiles. The activity of *Cg*CR decreased rapidly above 60 °C due to thermal inactivation. For *Dh*CR and *Cg*CR, the relative activities at 30 °C were 70.8% and 27.0% of the activity at the optimum temperature, respectively. Thermal stabilities were investigated at different temperatures. The half-lives of *Kt*CR, *Dh*CR and *Cg*CR at 30, 40 and 50 °C were 18, 462 and 169 h, 11.8, 111 and 80.6 h, and 0.16, 2.1 and 1.3 h, respectively, as shown in Table 3. *Dh*CR and *Cg*CR were stable at 30 and 40 °C, but unstable at higher

temperatures. The deactivation energies (E_a) of *Dh*CR, *Cg*CR and *Kt*CR were 218 ± 6, 198 ± 8, and 190 ± 8 kJ mol^{-1}, respectively. These results indicated that *Dh*CR and *Cg*CR were much more stable at room temperature than at elevated temperatures.[26]

The kinetic constants of the purified reductases for CAPE (**4**) and COBE (**22**) were calculated from the Lineweaver–Burk double-reciprocal plot, as shown in Table 3. The k_{cat} for **22** was 16.6 s^{-1} for *Dh*CR and 27.9 s^{-1} for *Cg*CR. Relative low K_M values for NADPH (<50 μM) for *Dh*CR and *Cg*CR guaranteed high efficiency, even when no external cofactors were added (Table S3†). Although the k_{cat} values for **4** of *Dh*CR and *Cg*CR were lower than that of *Kt*CR, they were much more efficient in the asymmetric reduction of COBE and stable to high temperatures. Their substrate specificity and catalytic performance in the preparation of chiral halohydrins were investigated further.

Substrate profiles of stereocomplementary *Dh*CR and *Cg*CR

No activity with NADH but full activity with NADPH was detected using purified *Dh*CR and *Cg*CR (data not shown), indicating both were NADPH-dependent carbonyl reductases. Twenty-five prochiral ketones (**1** to **25**) with various substituents, covering aromatic and aliphatic ketones and β-ketoesters, were selected to characterize the substrate spectra of *Dh*CR and *Cg*CR.

As shown in Fig. 2, different substrate profiles were observed with *Dh*CR and *Cg*CR. Among the tested substrates, no clear preference was discovered for *Dh*CR, whereas *Cg*CR preferred β-ketoesters to aromatic and aliphatic ketones. In addition to the increase of side-chain length of aromatic ketones, from acetophenone to 1-butyrophenone (**1**–**3**), the specific activity of *Dh*CR gradually decreased. *Cg*CR displayed higher catalytic activity for 1-butyrophenone than for 1-propiophenone. Due to the electron-imbalance, α-substituted acetophenone derivatives (**4**–**6**, **9**–**12**) were more easily reduced by reductases. Although CN was a strong electron-withdrawing group, benzoylacetonitrile (**6**) was difficult to reduce because of the steric hindrance of the CN group. 2′-Chloroacetophenone (**7**) was generally a poor substrate for carbonyl reductases. However, *Cg*CR displayed higher activity toward **7**. The specific activity ratio of 4′-chloroacetophenone (**8**) to **7** for *Cg*CR was 3.2, much lower than 88.3 for *Dh*CR, indicating that *Cg*CR could accept much larger aromatic ketones with *ortho* substituents on the phenyl ring. Compared with aryl ketones, heteroaryl ketones were more

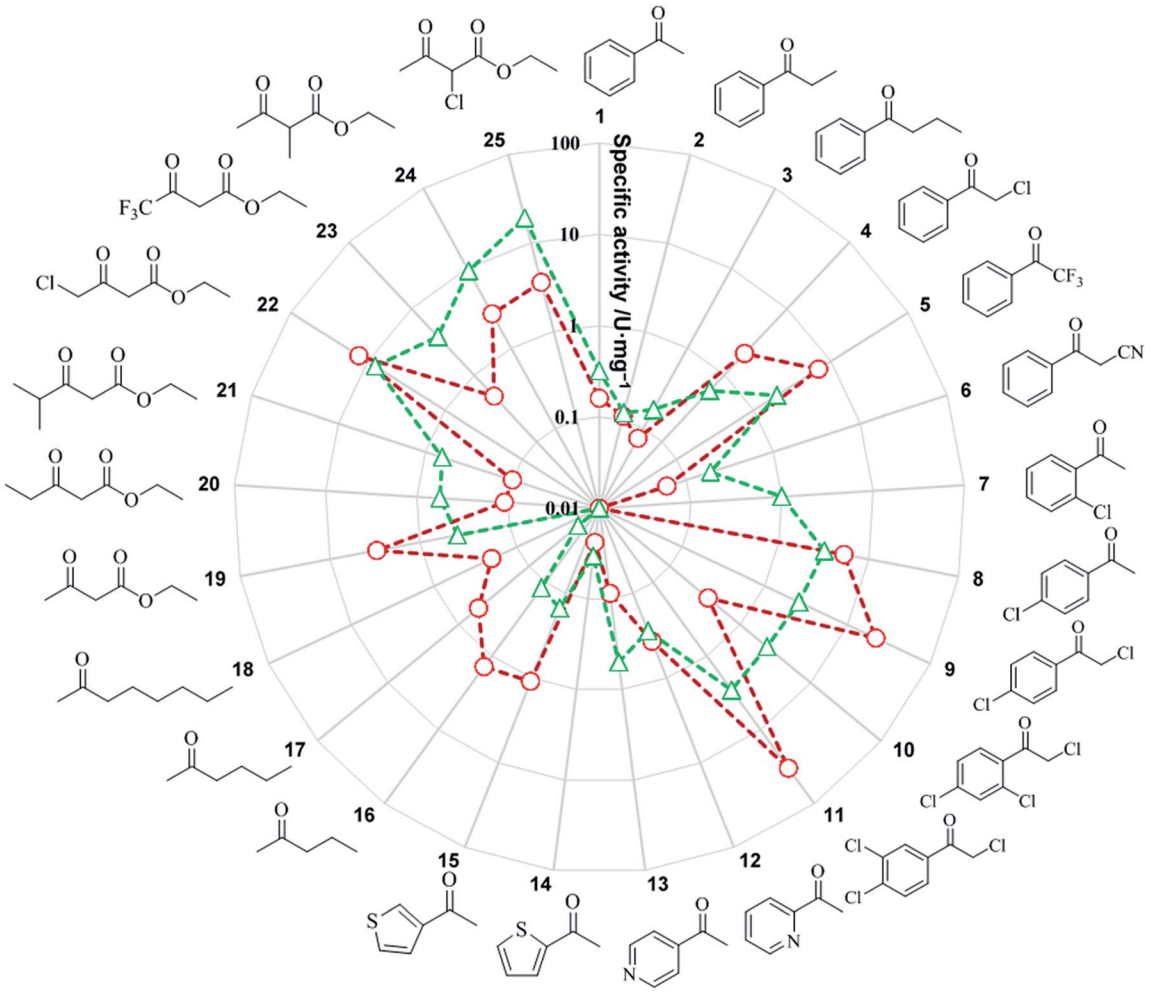

Fig. 2 Substrate profiles of *Dh*CR (○) and *Cg*CR (Δ). Specific activities are shown in logarithmic form in the spider web diagram. The activities equal to or lower than 0.01 U mg^{-1} purified protein are shown as 0.01 U mg^{-1}. Values are listed in Table S4 in ESI.†

difficult to reduce. Aliphatic ketones were better substrates for *Dh*CR than for *Cg*CR, suggesting that *Dh*CR could be used to prepare chiral aliphatic secondary alcohols. *Cg*CR showed higher activity to β-ketoesters than *Dh*CR, especially to ethyl 4,4,4-trifluro-3-oxo-butonate (**23**). The highest activity of *Dh*CR was found towards 2,3′,4′-trichloroacetophenone (**11**, 33 U mg^{-1}). Ethyl 2-chloro-3-oxo-butonate (**25**, 19 U mg^{-1}) was the best of the tested substrates for *Cg*CR. Interestingly, *Dh*CR showed the opposite enantioselectivity to *Cg*CR, although low enantioselectivity was observed with *Cg*CR for several substrates (20–98% ee, Table S4†). In the asymmetric reduction of prochiral ketones, *Dh*CR obeyed the anti-Prelog rule whereas *Cg*CR complied with Prelog priority. The preparation of both enantiomers of chiral α-halohydrins, which are usually of equal importance, could be achieved with these two stereocomplementary reductases.

In the regions conserved between *Dh*CR and *Cg*CR proteins, which are members of the SDR and AKR families, respectively, typical SDR and AKR sequence motifs, such as cofactor binding, catalytic, substrate binding and structure stabilizing residues, were found, as illustrated in Table S1 and Fig. S4 and S5.†[27] This also indicated that *Dh*CR and *Cg*CR belonged to the SDR and AKR families, respectively. Further consensus analysis with homologous proteins showed that they were members of the SDR51C and AKR1B10 subfamilies, based on online database nomenclature searches (http://www.sdr-enzymes.org/, http://www.med.upenn.edu/akr/).[28]

A characteristic glycine-rich Rossmann-fold scaffold was found in the *N*-terminal of *Dh*CR for binding the $NADP^+$ dinucleotide.[29] The Rossmann-fold sequence in *Dh*CR was TGSSGGIGWA, sharing the motif of the classical or extended subfamily. The length of the extended subfamily is 30 residues longer than the 250 amino acid residues of the classical SDR, and *Dh*CR also had the conserved adenine ring binding and active site motifs of the extended subfamily (Table S2†), *Dh*CR was a member of the extended group.

No Rossmann-fold scaffold motif was found in *Cg*CR. However, as shown in Table S1,† typical motifs for AKR were found in *Cg*CR, which indicated that *Cg*CR was a potential member of AKR superfamily.[30] Among the consensus sequences, the catalytic tetrad, Asp-Tyr-Lys-His (50-55-80-111), appeared in the *N*-terminal of *Cg*CR. Thr26, Asp50, Asn167, Gln190, Ser263 and Arg268 played important roles in cofactor binding. Other residues, such as Gly23, Gly25, Gly45, Asp106, Pro113, Gly165 and Pro187, might play a structural role in forming the barrel core, because they were found in the β-strand, α-helix and short loop regions of the barrel.

Optimization of the asymmetric reduction of COBE to chiral CHBEs

*Dh*CR and *Cg*CR were coexpressed with glucose dehydrogenases separately to provide cofactor regeneration systems. The catalytic performance in the asymmetric reduction of COBE (**22**) into optically active CHBE with *Dh*CR and *Cg*CR was systematically studied as shown in Table S6.† *Dh*CR could asymmetrically reduce substrate **22** into (*S*)-CHBE, an important synthon for statin side chains. In contrast, (*R*)-CHBE was produced with *Cg*CR as an intermediate for L-carnitine **22**, and was not stable in the aqueous phase, especially under alkaline conditions, and may be toxic to biocatalysts.[31] Biphasic systems are usually used to minimize the loss of the substrate and product. In the toluene/aqueous system, the partition coefficients of **22** and CHBE were 21.3 and 2.8, respectively, and *Dh*CR, *Cg*CR and *Bm*GDH retained their high activity; therefore, toluene was selected as the organic phase.[25] The intracellular amount of $NADP^+$ was also quantified to calculate total turnover number (TTN) of these two complementary reductases. There was 1.86 ± 0.13 μmol g^{-1} $NADP^+$ in DCW of *E. coli* BL21 (Table S5†), which was slightly higher than the reported amount of 0.39–0.79 μmol g^{-1} $NADP^+$ in DCW.[32] Less than 0.1 μmol g^{-1} of NADPH was detected, whereas 0.44 ± 0.02 μmol g^{-1} NAD^+ in DCW was calculated *in vivo* for *E. coli* BL21. There was less of a difference between *E. coli* BL21 harbouring *Dh*CR and *Cg*CR coding genes.

High substrate loading is desirable for practical applications, usually at more than 100 g L^{-1}. Hence, optimization was carried out to increase the substrate concentration and TTN of reductases in the toluene/aqueous biphasic system. Within 6 h, 0.2 M of **22** was asymmetrically reduced with >99% conversion by using 10 g L^{-1} *Dh*CR and 5 g L^{-1} *Cg*CR. In addition to the increase of the substrate/catalyst ratio, as much as 330 g L^{-1} (660 g L^{-1} in the toluene phase) of **22** could be fully reduced with no addition of an external cofactor (Table S6†). The preparation of (*S*)- and (*R*)-CHBE was scaled up to 1 L, and 330 g of **22** were added to the 0.5 L toluene phase and fully reduced within 24 h (Fig. 3). After purification, the molar isolation yield of (*S*)- and (*R*)-CHBE was calculated to be 92.5% and 93.0% respectively, ee_p was >99%. The substrate/catalyst (S/C) ratio was 33 for *Cg*CR and 16.5 for *Dh*CR.

As shown in Fig. 4 and Table S7,† much research has focused on the preparation of (*S*)-CHBE, because of its widespread use in the preparation of statin side-chains in the pharmaceutical industry. All the reductases that produced (*S*)-isomers belonged to the SDR family. Except for CmMR from *Candida magnolia*, most reductases displayed excellent enantioselectivity. The

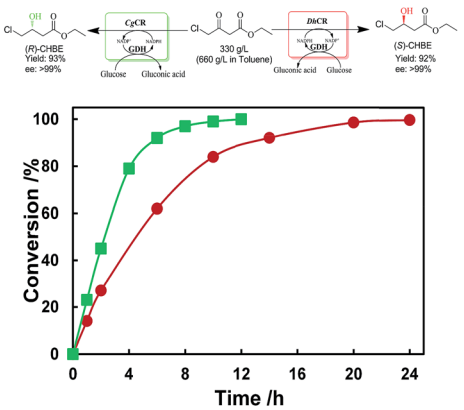

Fig. 3 Asymmetric reduction of 330 g COBE to both enantiomers of chiral CHBE with *Dh*CR and *Cg*CR in a 1 L reaction mixture (toluene/aqueous biphasic system).

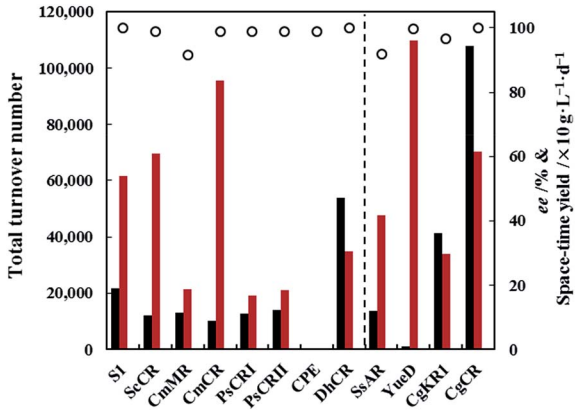

Fig. 4 Comparison of the catalytic performance of selected ketoreductases in the asymmetric reduction of COBE to chiral CHBE. Black bar (■): total turnover number, red bar (■): space-time yield, blank circle (○): ee.

highest substrate loading and TTN of the cofactor were achieved with carbonyl reductase *Sc*CR and CmS1 from *Streptomyces coelicolor* and *C. magnolia*.[15,31,33] However, the requirement for an external cofactor is a disadvantage for its wide use in organic synthesis.

With no exogenous $NADP^+$, as much as 330 g L^{-1} of the substrate could be asymmetrically reduced within 24 h using recombinant *Dh*CR, which provided a much more efficient and environmentally friendly reductase for preparing chiral (*S*)-CHBE. The TTN and space-time yield (STY) of *Dh*CR was 53 800 and 305 g L^{-1} day^{-1}, respectively, calculated based on intracellular $NADP^+$/NADPH. Compared with (*S*)-isomers, fewer reductases have been reported for producing (*R*)-CHBE. A carbonyl reductase from *Sporobolomyces salmonicolor*, *Ss*CR, could catalyze the full reduction of 300 g L^{-1} of **22**, with only 91.7% (*R*) ee.[34] Of the reductases that produce (*R*)-isomers, the gene YueD from *Bacillus subtilis* was reported to show the highest ee value at a substrate loading of 214 g L^{-1} (fed-batch). However, it required 1 mM $NADP^+$,[35] which would increase its cost and hinder its application. With no external cofactors, 330 g L^{-1} of **22** was asymmetrically reduced to optically pure (*R*)-CHBE, and the S/C, TTN and STY of *Cg*CR were 33 108 000 and 614 g L^{-1} day^{-1}, respectively.

Enzymatic preparation of both halohydrin enantiomers

High substrate specificity is an important characteristic of biocatalysts. Different substituents at different positions may imbue substrates with distinct electronic, hydrophobic, polar, and spatial properties. Unlike classical chemical catalysts, there

Table 4 Efficient bioreductive preparation of various chiral halohydrins at high substrate loading

Substrate	*Dh*CR					*Cg*CR					Chiral blocks in pharmaceutically relevant products
	Concn. [g L^{-1}]	Catal.[a] [g L^{-1}]	Time [h]	Yield [%]	ee [%], *R*/*S*	Concn. [g L^{-1}]	Catal.[b] [g L^{-1}]	Time [h]	Yield [%]	ee [%], *R*/*S*	
4	100	30	24	88	>99/*S*	30.8	20	24	85	98/*R*	Sotalol
5	174	30	24	90	>99/*S*	—[c]	—	—	—	—	Anticonvulsant
9	189	30	24	89	>99/*S*	94.5	20	24	90	>99/*R*	β3-Adrenoceptor
10	44.4	30	12	89	>99/*S*	100	20	12	88	>99/*R*	Econazole
11	100	30	12	90	>99/*S*	100	20	24	87	>99/*R*	Zoloft
22	330 (660)[d]	20	24	92	>99/*S*	330 (660)[d]	10	12	93	>99/*R*	Lipitor
23	184	30	24	89	>99/*S*	184	10	24	92	>99/*R*	Befloxatone

[a] Catalyst, dry cells of recombinant *E. coli* BL21/pET28-bmgdh-dhcr. [b] Catalyst, dry cells of recombinant *E. coli* BL21/pET28-bmgdh-cgcr. [c] Reaction was not performed due to the low ee value (54%). [d] 330 g L^{-1} in the reaction mixture and 660 g L^{-1} in organic phase.

are marked differences between biocatalysts for diverse substrates. The catalytic activity and enantioselectivity may vary according to changes in substrates. An ideal reductase should display high activity, enantioselectivity, and substrate tolerance, and, most importantly, a broad substrate scope. Although it is impossible to find one enzyme for all substrates, as an alternative tool in the organic synthesis of chiral compounds, a series of substrates containing similar functional groups should be catalyzed. Several α-substituted prochiral ketones with high activity and enantioselectivity in the substrate spectra analysis of *Dh*CR and *Cg*CR were chosen to test their applicability.

All the tested substrates were reduced at 100 g L^{-1} substrate loading to optically pure α-halohydrins as illustrated in Table 4. All the α-halohydrins are important chiral building blocks with pharmaceutical relevance. For example, (*S*)-α-chloro-1-acetophenol could be used for sotalol,[36a] (*S*)-2,2,2-trifluroacetophenol for liquid crystals and anticonvulsant pharmaceuticals,[36b,c] (*S*)-2,4′-dichloroacetophenol for adrenergic receptor agonists,[36d] (*S*)-2,3′,4′-trichloroacetophenol for sertraline,[36e] (*R*)-2,2′,4′-trichloroacetophenol for econazole,[5] and ethyl (*R*)-4,4,4-trifluro-3-hydroxybutyrate for befloxatone.[36f] The efficient preparation of optically pure α-halohydrins shows that *Dh*CR and *Cg*CR are promising catalytic enzymes.

Conclusions

In summary, two robust haloketone reductases (*Dh*CR and *Cg*CR) were identified from the recently developed carbonyl reductase toolbox through rescreening and characterization. Activity and enantioselectivity are usually the key criteria for chiral biocatalysis. In previous work, the carbonyl reductase *Kt*CR was discovered with high activity and enantioselectivity. However, 29 other candidates were identified by reassessing the enzymatic properties. Hence, a three-round screening strategy was proposed to recheck the missed reductases. Ethyl 4-chloro-3-oxobutanate, a different haloketone from α-chloro-1-acetophenone, was used to retest all 30 reductases. Twelve were returned with activity of more than 0.5 U mg^{-1}. Five with high enantioselectivity were selected to go through the substrate tolerance assay. Only *Kt*CR, *Dh*CR and *Cg*CR were stable enough, and their enzymatic properties were compared. After rescreening their thermostability, *Dh*CR and *Cg*CR, which had opposite enantioselectivity for the asymmetric reduction of prochiral ketones, were identified. At a 1 L scale, both reduced 330 g of **22** into chiral CHBEs, with 92.5% and 93.0% yields, respectively, and >99% ee. The S/C ratios were 33 for *Cg*CR and 16.5 for *Dh*CR. Seven chiral halohydrins with pharmaceutical relevance were asymmetrically prepared. Our results provide key evidence for the stereocomplementary enzymes *Dh*CR and *Cg*CR as potential robust reductases in organic synthesis.

Experimental

Materials

Prochiral ketones were all from commercial sources (TCI and Aladdin Inc.). Strains used as genome donors were purchased from CGMCC. The pET28a vector was obtained from Novagen (Madison, WI, USA). Competent cells of *E. coli* strains, Dh5α and BL21(DE3), were purchased from Tiangen (Shanghai, China).

General remarks for gene cloning, expression and purification of proteins

Gene cloning and construction of recombinant plasmids (pET28a-CRs) was reported in our previous work.[18] The *E. coli* BL21(DE3) cells harbouring recombinant pET28a-CRs were cultivated at 37 °C in LB medium containing 50 μg mL^{-1} kanamycin. When the OD_{600} of the culture reached 0.5–0.6, IPTG was added to a final concentration of 0.3 mM, and cultivation was continued at 25 °C for a further 15 h. The recombinant *E. coli* BL21(DE3) cells were collected and purified as previously described.[16,18]

Co-expression of reductase and GDH

The genes coding for *Kt*CR, *Dh*CR and *Cg*CR with independent promoters were separately cut from pET28-*ktcr*, pET28-*dhcr*, pET28-cgcr with *Bgl*II and *Xho*I. The pET28-*bmgdh* vector was digested with *Bam*HI and *Xho*I. The fragments of *ktcr*, *dhcr* and *cgcr* with independent promoters were ligated with the linear pET28-*bmgdh* vector to form pET28-*bmgdh-ktcr*, pET28-bmgdh-dhcr and pET28-*bmgdh-cgcr* plasmids.[25] The resulting plasmids were transformed into *E. coli* BL21 and over-expressed as mentioned above.

Enzyme activity assay

Reductase activity was detected spectrophotometrically at 30 °C through monitoring the change of NAD(P)H absorbance at 340 nm. The reaction mixture consisted of 2 μmol substrate (**4** or **22**, unless otherwise stated), 0.1 μmol NADPH or NADH, 50 μmol sodium phosphate buffers (pH 6.5), and an appropriate amount of enzyme in a total volume of 1 mL. One unit of enzyme activity was defined as the amount of enzyme that catalyzed the oxidation of 1 μmol of NADPH per minute under these conditions.

Enzyme characterization

The optimum pH of *Kt*CR, *Dh*CR and *Cg*CR was determined in the following buffers (final concentration, 50 mM): sodium citrate (pH 4.0–6.0), sodium phosphate (pH 6.0–8.5), and glycine-NaOH (pH 8.5–10.0) using above mentioned enzyme activity assay protocol. The optimum temperature was determined under the standard conditions at various temperatures (25–80 °C). Thermal stability was determined by incubating the purified enzyme (0.1 mg mL^{-1}) at the desired temperature (30, 40 or 50 °C) followed by periodically measuring the residual activity. The kinetic constant analysis of the purified enzyme was performed as previously described.[15]

Conversion and enantioselectivity analysis

The enantioselectivity was determined by examining the reduction of prochiral ketones using an NADPH regeneration system consisting of purified reductase and externally added glucose dehydrogenase (GDH). The reactions were carried out

in a reaction mixture (0.4 mL) comprising 50 mM sodium phosphate buffer (pH 6.5), 10 mM carbonyl substrates, 0.2 U of the purified reductase, 0.4 U of *Bm*GDH, 20 mM glucose and 0.5 mM $NADP^+$ with shaking for 12 h at 30 °C and 900 rpm. Each reaction mixture was extracted twice with ethyl acetate. The conversion and ee value were determined by GC analysis equipped with a CP-Chirasil-DEX CB (Varian, USA; 25 m × 0.25 mm × 0.39 mm) column or HPLC analysis using a Chiralcel OD-H column (Daicel Co., Japan; 4.6 × 250 mm) as described in our previous work.[16,18]

Quantification of intracellular $NADP^+$/NADPH

The intracellular amount of $NADP^+$/NADPH of *E. coli* BL21 was quantified by using HPLC (Shimadzu 2010, Shimadzu Scientific Instruments, Japan) equipped with Shim-pack VP-ODS C18 column (Shimadzu Scientific Instruments, Japan; 4.6 × 250 mm). Dry cells (0.10 g) or wet cells (0.50 g) of *E. coli* BL21 harbouring pET28a-*bmgdh-dhcr* or pET28a-*bmgdh-cgcr* plasmids was weighed and fully dispersed in 10 mL KPB (pH 7.0, 10 mM). The mixture was disrupted with sonication (400 W, 3 s sonication, pause of 7 s) in an ice/water bath and centrifuged at 12 000 rpm for 30 min. After that, the upper aqueous phase was filtered, diluted, and injected into the HPLC, which was performed with 3% aqueous acetonitrile containing 0.025 mM *N*,*N*,*N*-triethylamine as the mobile phase at a flow rate of 1.0 mL min^{-1}, monitored at 254 nm, and at 30 °C. The retention times of NAD(H) and NADP(H) were analysed with standards, which were 4.785, 4.555, 7.371 and 8.639 min for $NADP^+$, NAD^+, NADH and NADPH, respectively, as shown in Fig. S3.†

General protocol for bioconversion

General protocol for the asymmetric reduction of **4** and **22** into optically active α-chloro-1-acetophenol (CAPL) and ethyl 4-chloro-3-hydroxybutanate (CHBE) was carried out with the whole cell reaction of *E. coli* harbouring pET28-*bmgdh-ktcr*, pET28-*bmgdh-dhcr* and pET28-*bmgdh-cgcr*. The reaction mixture consisted of 1.0 mmol sodium phosphate buffer (5–10 mL, pH 6.5), 2.0–20.0 mmol of substrates in toluene (5 mL), glucose (1.5 equiv.) and an appropriate amount of dry cells as listed in Table S6.† The reaction was performed by magnetic agitation at 30 °C, 200 rpm and titrated with 2.0 M Na_2CO_3 to maintain the pH at 6.5 until termination. The reaction mixture was centrifuged (8000 × *g* for 5 min) to promote phase separation, and then the aqueous phase was saturated with NaCl and extracted with ethyl acetate three times. The organic phase was combined with extraction, dried over anhydrous Na_2SO_4 and evaporated under vacuum.

A 1 L reaction mixture of 20 g coexpressed *Bm*GDH and *Dh*CR or 10 g coexpressed *Bm*GDH and *Cg*CR dry cells, and glucose (30.0 g; 30.0 g portions were added at intervals) in 500 mL sodium phosphate buffer (0.1 M, pH 6.5) and an equal volume of toluene in a 3 L mechanically stirred tank reactor were pre-incubated at 30 °C for 10 min. The reaction was started by adding 330 g of **22**. The pH of the reaction mixture was kept at 6.5 with 2.0 M Na_2CO_3. After stirring at 120 rpm for 24 h, the mixture was extracted with 500 mL ethyl acetate three times. The organic phase was combined, dried over anhydrous Na_2SO_4 and evaporated under vacuum.

Asymmetric preparation of six α-halohydrins was conducted using the same protocol as COBE (**22**). The reaction mixture consisted of 1.0 mmol sodium phosphate buffer (5–10 mL, pH 6.5), 2.0–10.0 mmol of substrates in toluene (5 mL), glucose (1.5 equiv.) and appropriate amounts of dry cells as listed in Table 4. The reaction was performed with magnetic agitation at 30 °C, 200 rpm and titrated with 1.0 M Na_2CO_3 to keep the pH at 6.5 until completion. Reactions were stopped and extracted as above.

Acknowledgements

This work was financially supported by the National Natural Science Foundation of China (no. 21276082), Ministry of Science and Technology, P. R. China (nos 2011CB710800 and 2011AA02A210), China National Special Fund for State Key Laboratory of Bioreactor Engineering (no. 2060204) and Huo Yingdong Education Foundation.

Notes and references

1 (*a*) R. N. Patel, *ACS Catal.*, 2011, **1**, 1056–1074; (*b*) J. H. Tao and J. H. Xu, *Curr. Opin. Chem. Biol.*, 2009, **13**, 43–50; (*c*) J. Magano and J. R. Dunetz, *Org. Process Res. Dev.*, 2012, **16**, 1156–1184.

2 (*a*) Z. L. Wei, Z. Y. Li and G. Q. Lin, *Tetrahedron*, 1998, **54**, 13059–13072; (*b*) D. M. Zhu, C. Mukherjee and L. Hua, *Tetrahedron: Asymmetry*, 2005, **16**, 3275–3278; (*c*) N. Itoh, K. Isotani, M. Nakamura, K. Inoue, Y. Isogai and Y. Makino, *Appl. Microbiol. Biotechnol.*, 2012, **93**, 1075–1085.

3 H. Yamamoto, K. Mitsuhashi, N. Kimoto, N. Esaki and Y. Kobayshi, *Biosci., Biotechnol., Biochem.*, 2004, **68**, 638–649.

4 M. Kataoka, L. P. Rohani, K. Yamamoto, H. Kawabata, M. Wada, K. Kita, H. Yanase and S. Shimizu, *Appl. Microbiol. Biotechnol.*, 1999, **41**, 486–490.

5 J. Mangas-Sanchez, E. Busto, V. Gotor-Fernandez, F. Malpartida and V. Gotor, *J. Org. Chem.*, 2011, **76**, 2115–2122.

6 (*a*) A. Schmid, J. S. Dordick, B. Hauer, A. Kiener, M. Wubbolts and B. Witholt, *Nature*, 2001, **409**, 258–268; (*b*) P. T. Anastas and M. M. Kirchhoff, *Acc. Chem. Res.*, 2002, **35**, 686–694; (*c*) J. Clark, R. Sheldon, C. Raston, M. Poliakoff and W. Leitner, *Green Chem.*, 2014, **16**, 18–23.

7 (*a*) H. E. Schoemaker, D. Mink and M. G. Wubbolts, *Science*, 2003, **299**, 1694–1697; (*b*) R. E. Morris and X. H. Bu, *Nat. Chem.*, 2010, **2**, 353–361; (*c*) G. W. Zheng and J. H. Xu, *Curr. Opin. Biotechnol.*, 2011, **22**, 784–792.

8 (*a*) K. Nakamura, R. Yamanaka, T. Matsuda and T. Harada, *Tetrahedron: Asymmetry*, 2003, **14**, 2659–2681; (*b*) H. Gröger, F. Chamouleau, N. Orologas, C. Rollmann, K. Drauz, W. Hummel, A. Weckbecker and O. May, *Angew. Chem., Int. Ed.*, 2006, **45**, 5677–5681; (*c*) F. Hollmann, I. W. C. E. Arends and D. Holtmann, *Green Chem.*, 2011, **13**, 2285–2313.

9 U. T. Bornscheuer, G. W. Huisman, R. J. Kazlauskas, S. Lutz, J. C. Moore and K. Robins, *Nature*, 2012, **485**, 185–194.

10 C. C. C. R. de Carvalho, *Biotechnol. Adv.*, 2011, **29**, 75–83.

11 (*a*) G. A. Behrens, A. Hummel, S. K. Padhi, S. Schatzle and U. T. Bornscheuer, *Adv. Synth. Catal.*, 2011, **353**, 2191–2215; (*b*) T. Davids, M. Schmidt, D. Bottcher and U. T. Bornscheuer, *Curr. Opin. Chem. Biol.*, 2013, **17**, 215–220.

12 I. Pagani, K. Liolios, J. Jansson, I. M. A. Chen, T. Smirnova, B. Nosrat, V. M. Markowitz and N. C. Kyrpides, *Nucleic Acids Res.*, 2012, **40**, D571–D579.

13 (*a*) S. Z. Zhu, C. Y. Gong, D. W. Song, S. H. Gao and G. J. Zheng, *Appl. Environ. Microbiol.*, 2012, **78**, 7492–7495; (*b*) M. Begley, P. D. Cotter, C. Hill and R. P. Ross, *Appl. Environ. Microbiol.*, 2009, **75**, 5451–5460.

14 S. Luetz, L. Giver and J. Lalonde, *Biotechnol. Bioeng.*, 2008, **101**, 647–653.

15 (*a*) L. J. Wang, C. X. Li, Y. Ni, J. Zhang, X. Liu and J. H. Xu, *Bioresour. Technol.*, 2011, **102**, 7023–7028; (*b*) J. Pan, G. W. Zheng, Q. Ye and J. H. Xu, *Org. Process Res. Dev.*, 2014, **18**, 739–743.

16 H. M. Ma, L. L. Yang, Y. Ni, J. Zhang, C. X. Li, G. W. Zheng, H. Y. Yang and J. H. Xu, *Adv. Synth. Catal.*, 2012, **354**, 1765–1772.

17 N. D. Shen, Y. Ni, H. M. Ma, L. J. Wang, C. X. Li, G. W. Zheng, J. Zhang and J. H. Xu, *Org. Lett.*, 2012, **14**, 1982–1985.

18 G. C. Xu, H. L. Yu, X. Y. Zhang and J. H. Xu, *ACS Catal.*, 2012, **2**, 2566–2571.

19 W. X. Zhang, G. C. Xu, L. Huang, J. Pan, H. L. Yu and J. H. Xu, *Org. Lett.*, 2013, **15**, 4914–4919.

20 J. Li, J. Pan, J. Zhang and J. H. Xu, *J. Mol. Catal. B: Enzym.*, 2014, **105**, 11–17.

21 H. H. Nguyen-Tran, G. W. Zheng, X. H. Qian and J. H. Xu, *Chem. Commun.*, 2014, **50**, 2861–2864.

22 B. D. Ma, H. L. Yu, J. Pan, J. Y. Liu, X. Ju and J. H. Xu, *Bioresour. Technol.*, 2013, **133**, 354–360.

23 C. S. Zhang, Z. J. Zhang, C. X. Li, H. L. Yu, G. W. Zheng and J. H. Xu, *Appl. Microbiol. Biotechnol.*, 2012, **95**, 91–99.

24 J. Y. Liu, G. W. Zheng, T. Imanaka and J. H. Xu, *Biotechnol. Bioprocess Eng.*, 2014, **19**, 442–448.

25 G. C. Xu, H. L. Yu, Z. J. Zhang and J. H. Xu, *Org. Lett.*, 2013, **15**, 5408–5411.

26 Y. P. Xu, Y. H. Guan, H. L. Yu, Y. Ni, B. D. Ma and J. H. Xu, *J. Mol. Catal. B: Enzym.*, 2014, **104**, 108–114.

27 (*a*) R. D. Mindnich and T. M. Penning, *Hum. Genomics*, 2009, **3**, 362–370; (*b*) B. Persson and Y. Kallberg, *Chem.-Biol. Interact.*, 2013, **202**, 111–115.

28 (*a*) D. Hyndman, D. R. Bauman, V. V. Heredia and M. Penning, *Chem.-Biol. Interact.*, 2003, **143–144**, 621–631; (*b*) B. Persson, Y. Kallberg, J. E. Bray, E. Bruford, S. L. Dellaporta, A. D. Favia, R. G. Duarte, H. Jörnvall, K. L. Kavanagh, N. Kedishvili, M. Kisiela, E. Maser, R. Mindnich, S. Orchard, T. M. Penning, J. M. Thornton, J. Adamski and U. Oppermann, *Chem.-Biol. Interact.*, 2009, **178**, 94–98.

29 C. Filling, K. D. Berndt, J. Benach, S. Knapp, T. Prozorovski, E. Nordling, R. Ladenstein, H. Jörnvall and U. Oppermann, *J. Biol. Chem.*, 2002, **277**, 25677–25684.

30 L. Di Costanzo, T. M. Penning and D. W. Christianson, *Chem.-Biol. Interact.*, 2009, **178**, 127–133.

31 N. Kizaki, Y. Yasohara, J. Hasegawa, M. Wada, M. Kataoka and S. Shimizu, *Appl. Microbiol. Biotechnol.*, 2001, **55**, 590–595.

32 (*a*) Z. J. Li, L. Cai, Q. Wu and G. Q. Chen, *Appl. Microbiol. Biotechnol.*, 2009, **83**, 929–947; (*b*) H. C. Lee, J. S. Kim, W. Jang and S. Y. Kim, *J. Biotechnol.*, 2010, **149**, 24–32.

33 Y. C. He, Z. C. Tao, X. Zhang, Z. X. Yang and J. H. Xu, *Bioresour. Technol.*, 2014, **161**, 461–464.

34 M. Kataoka, L. P. Rohani, K. Yamamoto, H. Kawabata, M. Wada, K. Kita, H. Yanase and S. Shimizu, *Appl. Microbiol. Biotechnol.*, 1999, **41**, 486–490.

35 Y. Ni, C. X. Li, L. J. Wang, J. Zhang and J. H. Xu, *Org. Biomol. Chem.*, 2011, **9**, 5463–5468.

36 (*a*) M. Kapoor, N. Anand, K. Ahmad, S. Koul, S. S. Chimni, S. C. Taneja and G. N. Qazi, *Tetrahedron: Asymmetry*, 2005, **16**, 717–725; (*b*) T. Fujisawa, K. Ichikawa and M. Shimizu, *Tetrahedron: Asymmetry*, 1993, **4**, 1237–1240; (*c*) J. Nie, H. C. Guo, D. Cahard and J. A. Ma, *Chem. Rev.*, 2011, **111**, 455–529; (*d*) H. Lin, Y. Z. Chen, X. Y. Xu, S. W. Xia and L. X. Wang, *J. Mol. Catal. B: Enzym.*, 2009, **57**, 1–5; (*e*) P. Krumlinde, K. Bogar and J. E. Bäckvall, *Chem.–Eur. J.*, 2010, **16**, 4031–4036; (*f*) X. Rabasseda, L. A. Sorbera and J. Castaner, *Drugs Future*, 1999, **24**, 1057–1067.